TECHNICAL UNIVERSITY OF CLUJ-NAPOCA

ACTA TECHNICA NAPOCENSIS

Series: Applied Mathematics, Mechanics, and Engineering
Vol. 66, Issue IV, November, 2023

DETERMINATION OF LIGNITE SHEAR STRENGTH ALONG AN IMPOSED PLANE BY SIMULATION AND MODELLING USING FDEM

Florin Dumitru POPESCU, Ciprian-Gheorghe DANCIU, Andrei ANDRAȘ, Ildiko BRÎNAȘ, Sorin Mihai RADU, Mirela Ancuța NEAGA (RADU)

Abstract: FDEM (Finite Discrete Element Method) is a computational numeric method [1-3] that permits dynamic simulation of the interaction of several bodies. Thus, when meeting a fracture criterion, bodies can elastically deform, have translational and rotational movements, interact and fracture. These processes lead to the formation of other discrete bodies which in turn can undergo movements, interactions, deformations and fractures. The Geomechanica IRAZU software package used to perform all simulations within this paper is based on the FDEM concept, thus being a versatile tool for simulations specific to rock mechanics. In the paper a computerised simulation of the shear strength test along an imposed plane was conducted for lignite. In order to achieve this, a series of theoretical aspects regarding shear strength were presented, along with standardized shear testing methods, as well as the steps to be followed to simulate the shear strength test.

Keywords: *lignite, shear strength, simulation, imposed plane, virtual specimen, FDEM, IRAZU.*

1. MINEFIELD SHEAR STRENGTH

When unbroken rock is submitted to shear, the shear stress raises rapidly until the maximum shear strength is attained thus initiating slippage on the plane of fracture. As the displacement advances, there is a smoothing of the fracture plane surfaces, resulting in reduction of shear strength to a residual value depending on the residual friction angle ϕ_r, and the residual cohesion c_r. The residual cohesion is negligeable (0.1 MPa) for most rocks [4], so usually it's considered nil. In geo-engineering, this residual shear strength is essential as rock mass, although already containing fracture surfaces, must remain functional and safe, being subject to further fractures due to stresses activated by mining. Ante– and post–rupture analysis is made harder by discontinuities, irregular natural surface shapes and the presence of fluids.

The pattern of the ripples on the natural discontinuities as a form of mechanical interlocking is shown in Figure 1. Shear displacement can occur in two modes: the first, where opposite surfaces move on top of each other causing the expansion of the rock mass, thus volume increase and additional frictional resistance appears; the second, involves breaking the ripples between the two surfaces, thus we are dealing with an extra element of unbroken cohesion.

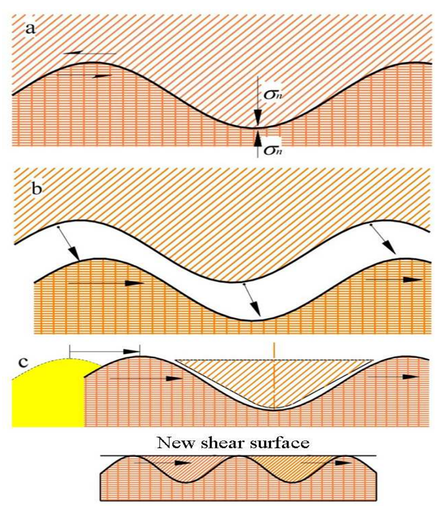

Fig.1. Pattern of ripples on natural fractures as a type of mechanical interlocking. **a).** No relative displacement between layers. Until shear failure, surfaces are kept together by friction, cohesion, and strength of surfaces in contact; **b).** Reciprocal movement between layers due to their separation; **c).** Reciprocal movement between layers due to overcoming contact forces of rock surfaces (Based on [5])

Received: 16.08.23; **Similarities**: 04.10.23: **Reviewed**: 26.10./01.11.23: **Accepted**:21.11.23.

This additional cohesion is depending on the contact strength of the rock encompassing the surface ripples. As determined by experiments [6, 7], equation 1 expresses frictional resistance:

$$\tau_r = \sigma_n \tan\left(\phi_b + i\right) \quad (1)$$

where τ_r is the residual shear strength, ϕ_b is the basic angle of friction, and i is the angle of the saw tooth face of the corrugation.

2. SHEAR STRENGTH TEST ALONG AN IMPOSED BREAKING PLANE

This type of test [8-10] involves the application of a tangential force to a rock specimen, acting on an imposed breaking plane which results from the test conditions. Thus, the shear strength determined is an average value depending on the shape of the specimen, the testing device, and the test conditions.

The specimens [11] are cylindrical with a diameter and height of 42 mm, with differences of up to ±0.25 mm allowed for each. In order to ensure their base parallelism and axis perpendicularity, their processing is done on a lathe, with a maximum deviation of ±0.02 mm. The testing device (see Figure 2) is made of several parts: shear box (1), split mould with various inclination (2), wedge (3), platen (4), rail bearing (5). For this testing the inclinations of the split mould have angles of 30º, 45º and 60º.

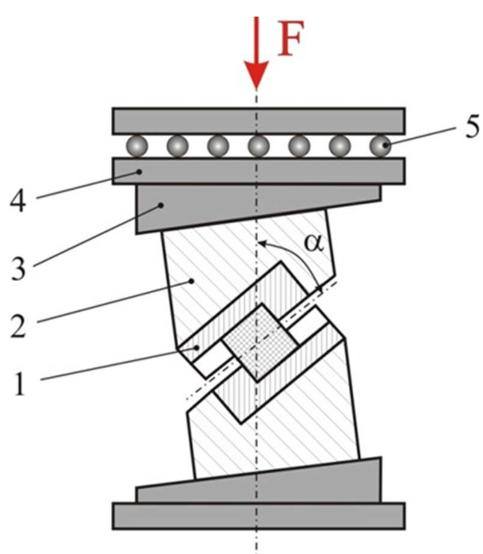

Fig.2. The shear strength along an imposed breaking plane testing device

Performing the test involves adjustments of the testing device to meet the chosen load range. The press must develop a progressive and uniform compression load of 5–10 daN/cm^2 per second until failure, thus determining the maximum load to failure F_r. The shear strength along an imposed breaking plane is calculated as:

$$\tau_{rf\alpha} = \frac{F_r}{A_0} \cdot \cos\alpha \quad [\text{daN/cm}^2] \quad (2)$$

where $\tau_{rf\,a}$ is the shear strength along an imposed plane for angle α, F_r (in daN) is the maximum load recorded at specimen failure, A_0 (in cm^2) is the initial area of the shear section, and α the angle between the breaking plane and the direction of force (in degrees).

The unit stress normal to the shear plane is:

$$\sigma_{rf\alpha} = \frac{F_r}{A_0} \cdot \sin\alpha \quad [\text{daN/cm}^2] \quad (3)$$

where $\sigma_{rf\,a}$ represents the unit stress, normal to the imposed shear plane for angle α, and F_r, A_0, α are the same as for equation 2.

3. KINEMATICS OF THE SHEAR TEST

Testing labs have different types of shear testing devices, for samples with shear surfaces up to 400 cm^2. Figure 3 shows the testing device from the Rock Mechanics Lab of the University of Petroșani, prepared for a shear test.

Fig.3. Testing device ready for shear test

For the device presented in figure 3, the lower platen moves vertically upwards at constant velocity and the upper platen is fixed. Direct shearing of the specimen is done by two shear boxes. One is driven vertically by the lower platen, while between the upper shear box and the upper platen there is a rail bearing that causes a horizontal movement of the upper shear box as a result of the pressure that the lower shear box exerts on it through the contact surfaces of the shear boxes. The relative movement between the contact surfaces of the shear boxes will cause the specimen to shear.

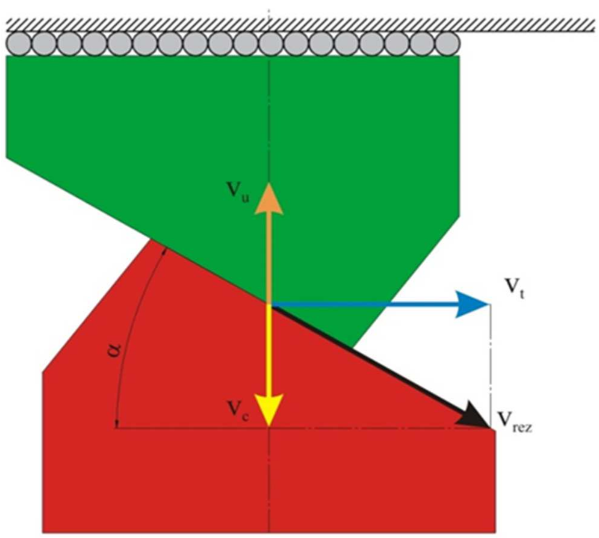

Fig.4. Kinematics of the shear test

A schematic image of shear kinematics is shown in figure 4, where it can be seen that the two shear boxes have the angle of inclination α. Assuming the velocity of the lower shear box v_u is known, the translation velocity v_t (horizontal velocity of the upper shear box), and the resultant velocity v_{rez} (shear velocity), can be calculated.

$$v_t = \frac{v_u}{\tan(\alpha)} \tag{4}$$

$$v_{rez} = \frac{v_u}{\sin(\alpha)} \tag{5}$$

$$v_c = v_u \tag{6}$$

Using equations (4) and (5), the variation of the translation v_t and resultant v_{rez} velocities function of the angle of inclination α were plotted as shown in figure 5. The velocity of the lower platen was considered v_u=0.05m/s. Analysis of the variation graphs of the two velocities, indicates that a larger inclination angle results in a lower shear rate, while a smaller inclination angle results in a higher shear rate.

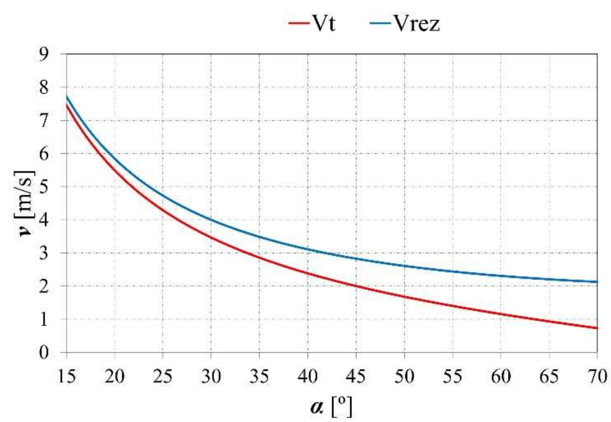

Fig.5. Variation of v_t and v_{rez} function of the angle α

4. MODELLING AND SIMULATION OF THE SHEAR STRENGTH ALONG AN IMPOSED PLANE AT A 30º ANGLE

For the shear test simulation in IRAZU, first the geometry of the model was created in SolidWorks [12]. The dimensions (Figure 6) of the model are average values based on the specimens cored at the Rock Mechanics Lab of the University of Petroşani. The geometry thus created was saved in .dxf format and imported in IRAZU.

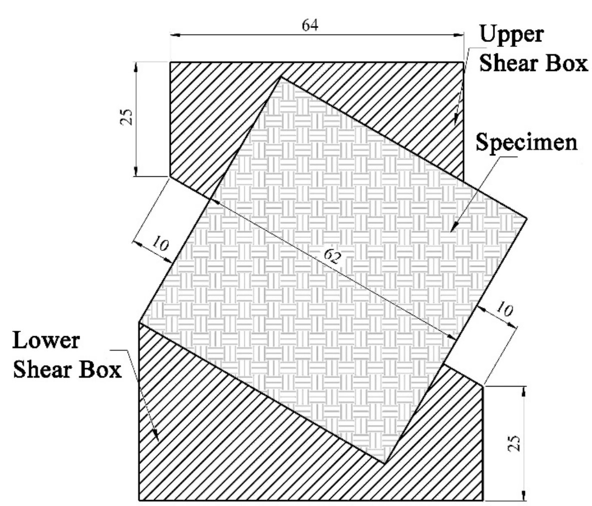

Fig.6. The geometry of the model and the key elements of the simulation

Also highlighted in Figure 6 are the three key elements for the simulation: the two shear boxes that produce the shear stress and the lignite specimen. Equation (4) imposes the values of the two velocities (translation and resultant), so that the inclined surfaces of the shear boxes are parallel with the shear plane throughout the simulation.

4.1. Set-up of the shear strength test simulation in IRAZU

After importing the geometry created in SolidWorks, the IRAZU model is setup [13]: both shear boxes, and the specimen were identified and selected. Next, the finite element size for each were defined, Gmsh app being used for generating the triangular finite element mesh shown in figure 7.

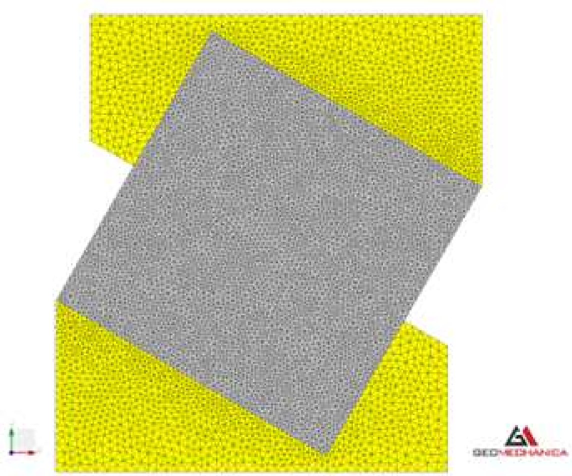

Fig.7. The finite element mesh generated for the model

The size of the finite element for the upper and lower shear boxes is 2 mm while the size of the finite element of the specimen is smaller, equal to 1 mm thus having a finer mesh.

4.2. Set-up of the shear strength test simulation parameters

4.2.1. The boundary conditions

For the model considered, the boundary conditions refer to the shear boxes. As mentioned before the lower shear box moves upwards vertically at a velocity of 0.05 m/s (constant) and imposes the upper shear box to move horizontally at a velocity of 0.087 m/s (contant), and as shown in figure 8.

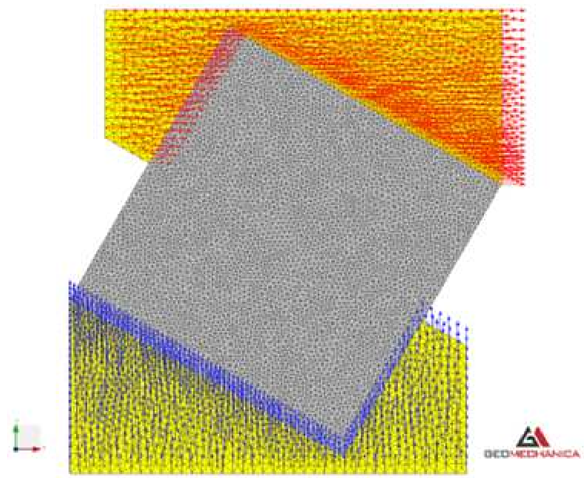

Fig.8. The boundary conditions

4.2.2 The material properties

Properties of the materials for the shear test simulation are referring to the shear boxes and the lignite specimen. For the shear boxes they are taken from the material library of IRAZU while for the lignite specimen they are defined based on geotechnical lab determinations, with values as presented in Table 1.

Table 1

Lignite specimen material properties

Elastic characteristics		
Density	Young modulus	Poisson coefficient
kg/m^3	Pa	-
1250	3.1×10^8	
Strength characteristics		
Friction coefficient	Cohesion	Tensile strength
-	Pa	Pa
	7×10^5	3.5×10^5

4.2.3. The calculation parameters

The calculation parameters of the shear test simulation refer to the number of iteration steps–3×10^6, the duration of an iteration step–2.5×10^{-6} seconds as well as to the sampling rate of the graphical response–20,000 steps.

5. RESULTS AND DISCUSSION

The outcomes of the lignite shear test simulation are presented using ParaView. Because of certain limitations of niche software like IRAZU to present the results in a graphically appealing way, in order to highlight the results post-processing engines are used. ParaView was chosen, as it is open-source, and a top post-processing visualization engine, fully integrated with the workflow and processes of IRAZU, and it allows quick and accurate analyse of obtained data and building of visualizations.

In order to simulate the lignite shear strength along an imposed breaking plane, the variation in time of the magnitude of the stress along a line parallel to the imposed breaking plane was plotted using the *Plot Over Line* filter of ParaView [14]. Figure 9 shows the line and its defining coordinates.

The distribution of the shear stress τ on the surface of the specimen and the finite element mesh nodes where the failure took place were highlighted in the left side of Figures 1, series a—j.

In the right side of the same figure series, the variation of the shear stress τ along the line parallel to the imposed breaking plane is presented for the entire simulation time.

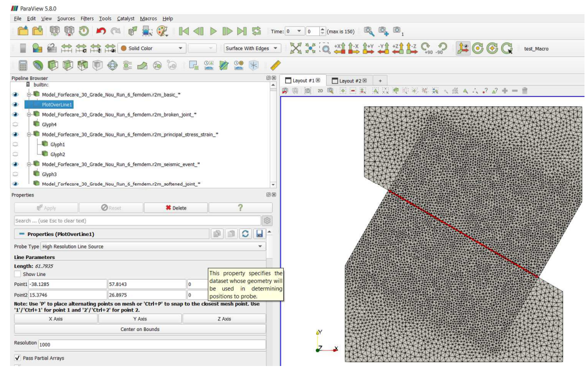

Fig.9. Plot Over Line filter and line used for the magnitude variation line plotting

By analysing the series of images in figure 10, it is seen that the shear stress has a concave parabolic shape along the line parallel to the imposed breaking plane.

The left part of the sequence of images clearly highlights the failure phenomenon, that initially occurs in the upper right and lower left of the specimen. These are superficial fractures, which could not be highlighted in the case of lab tests performed.

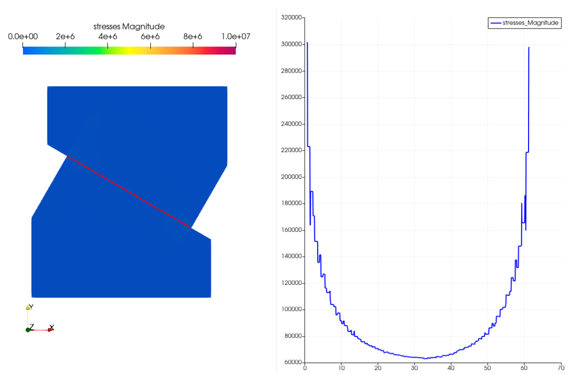

a).

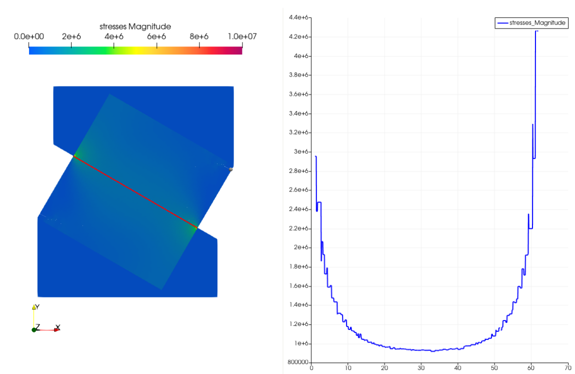

b).

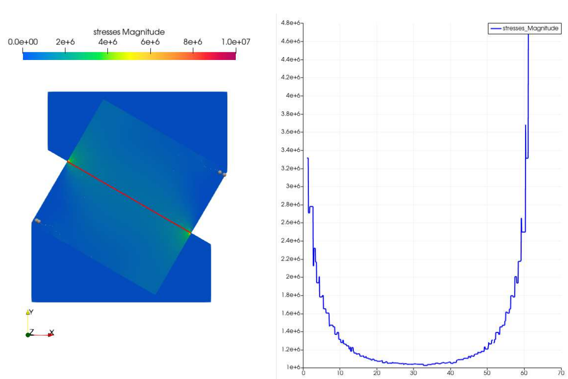

c).

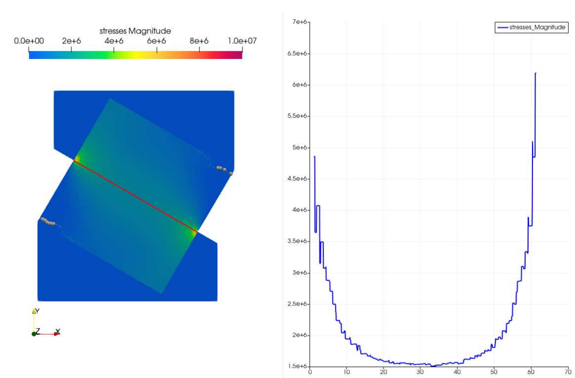

d).

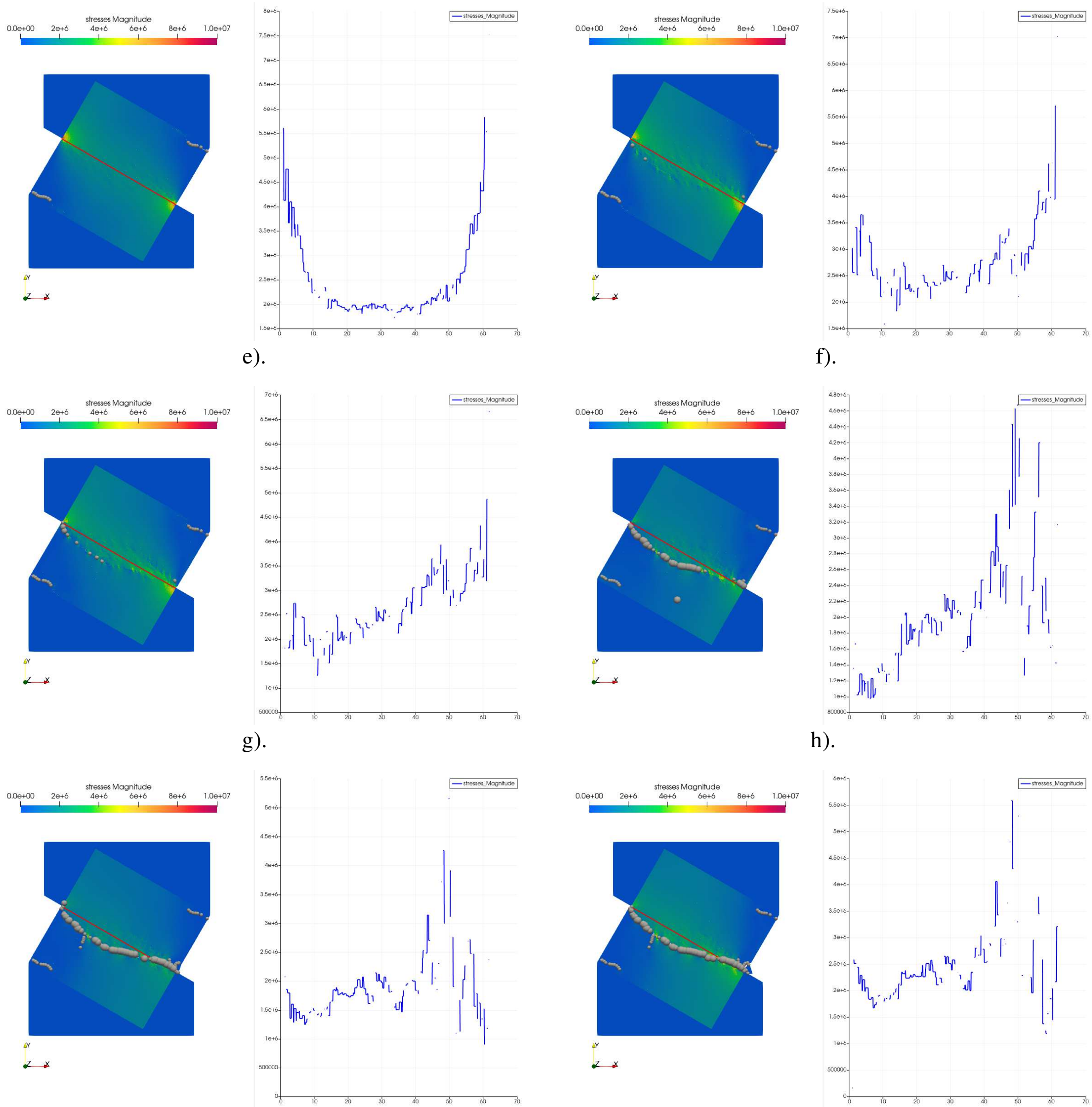

e). f). g). h). i). j).

Fig. 10. The distribution of the shear stress *τ* on the surface of the specimen and the finite element mesh nodes where the failure occurs (left part of each image), and the variation of the shear stress τ along the line parallel to the imposed breaking plane is presented for the entire simulation time (right part of each image)

Figure 11, series a—f shows the energy variation associated with the fracture phenomenon and the variation in the magnitude of the shear stress on the surface of the specimen during the shear strength test simulation along an imposed plane.

For these results, ParaView was used to calculate the maximum shear stress value of $\tau = 07.14 \times 10^6$ Pa.

6. CONCLUSIONS

The paper represents a part of the research results carried out by the team of authors within the VETAF-Geo research project. In essence, the research efforts were directed towards modelling and simulation with the IRAZU software package of the specific stresses in rock mechanics: compressive, direct and indirect tensile, and shear. The results obtained for simulating shear stress highlight the major role that computer simulation tools play in research activity and especially in analysing the behaviour of anisotropic materials such as lignite. The use of IRAZU software package represents a premiere at national level, and the results obtained, and their visualization—with special accent on the initiation and propagation of the fracturing phenomena with the help of ParaView—is also a modern teaching approach in rock mechanics and engineering.

ACKNOWLEDGEMENTS

This research has been conducted and funded by the University of Petroşani within the VETAF-Geo project.

7. REFERENCES

[1] Munjiza, A. *The Combined Finite-Discrete Element Method.* Hoboken: John Wiley & Sons, Hoboken, NJ, 333 pp, 2004.

[2] Mahabadi, O.K., Lisjak, A., Munjiza, A., Grasselli, G. *Y-Geo: New Combined Finite-Discrete Element Numerical Code for Geomechanical Applications.* International Journal of Geomechanics, 12, 676–688, 2012.

[3] Lisjak, A., Kaifosh, P., He, L., Tatone, B., Mahabadi, O. K., Grasselli, G. *A 2D, fully-coupled, hydro-mechanical, FDEM formulation for modelling fracturing processes in discontinuous, porous rock masses.* Computers and Geotechnics, 81, 1-18, 2017.

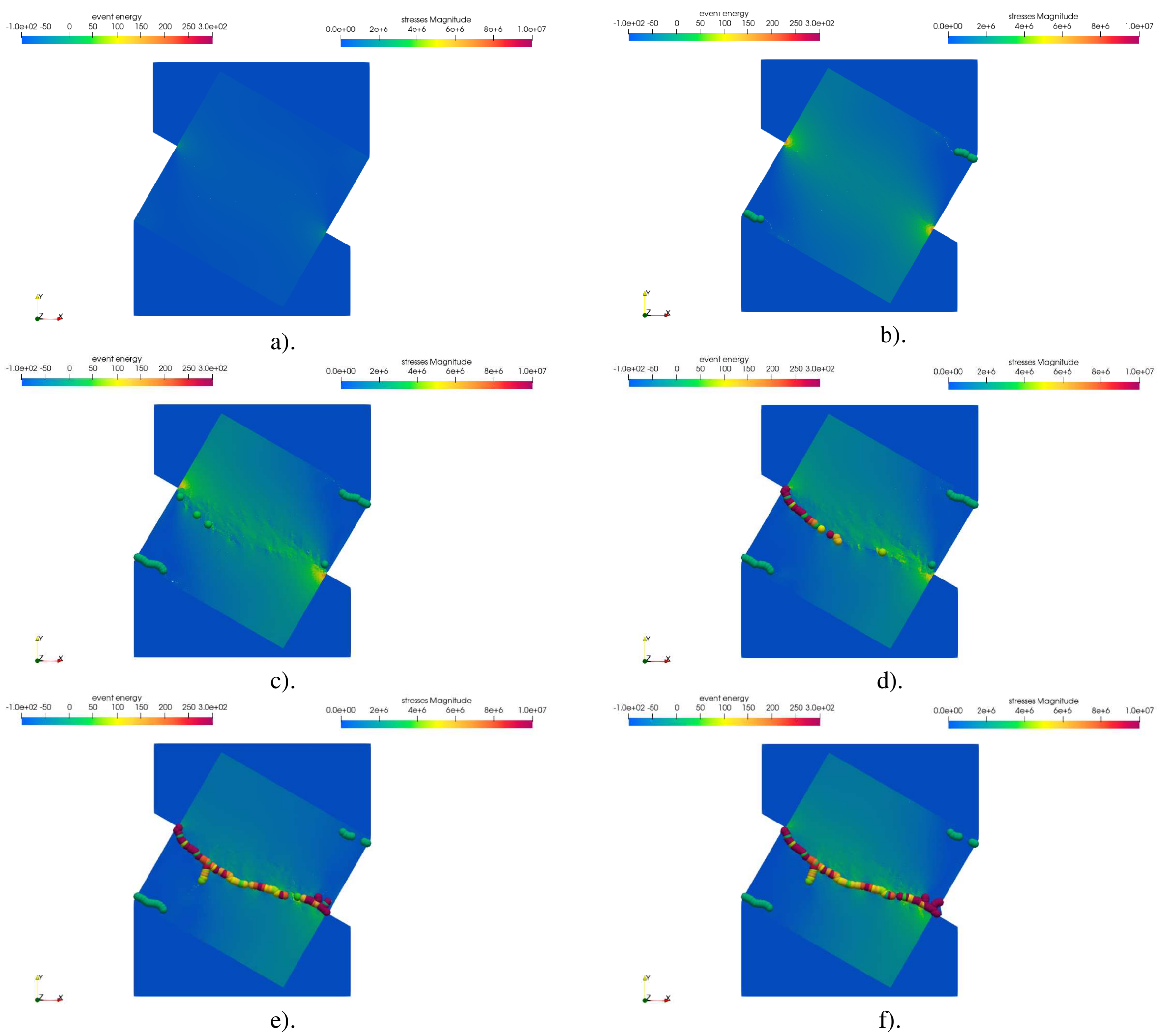

Fig. 11. The energy variation during fracture and the variation of the shear stress

[4] Cook, N.G.W., Klokow, J.W., White, A.J.A. *Practical rock mechanics for gold mining* (PRD series no. 167). Johannesburg: Chamber of Mines of South Africa, 1974.
[5] Galvin, J. M. *Ground engineering-principles and practices for underground coal mining.* Springer, 2016.
[6] Patton, F.D. *Multiple modes of shear failure in rock.* ISRM Congress. ISRM, 1966.
[7] Hoek, E., Kaiser, P.K., Bawden, W.F. *Support of Underground Excavations in Hard Rock.* CRC Press, 2000. https://doi.org/10.1201/b16978
[8] Backers, T., Stephansson, O. *ISRM Suggested Method for the Determination of Mode II Fracture Toughness.* Rock Mech Rock Eng, 45, 1011–1022, 2012. doi.org/10.1007/s00603-012-0271-9
[9] Muralha, J., Grasselli, G., Tatone, B., Blümel, M., Chryssanthakis, P., Yujing, J. *ISRM suggested method for laboratory determination of the shear strength of rock joints: revised version*. Rock Mech Rock Eng, 47, 291-302. 2014. doi.org/10.1007/s00603-013-0519-z
[10] Danciu, C. *Mecanica rocilor,* Editura Universitas, Petroşani, 2011.
[11] *ASTM D4543-08 standard practice.* American Society for Testing and Materials (ASTM) International, 2008.
[12] Popescu, F. D., Radu, S.M., Andras, A., Kertesz, I. *Infografică, modelare şi simulare asistată de calculator*, Editura Universitas, Petroşani, 2020.
[13] Geomechanica Inc, *Irazu 2D Geomechanical Simulation Software. V. 5.1.* Theory Manual, 2022.
[14] Ayachit, U. *The ParaView Guide: A Parallel Visualization Application*, Kitware, 2015.

Simularea și modelarea prin metoda elementelor finite discrete a solicitării la forfecare a lignitului după un plan de rupere obligat

Rezumat: Metoda combinată a elementelor finite-discrete (FDEM), este o metodă numerică de calcul care permite simularea dinamică a interacțiunii mai multor corpuri. Astfel la îndeplinirea unui criteriu de fracturare corpurile se pot deforma elastic, pot avea mișcări de translație și de rotație, pot interacționa și se pot fractura. Aceste procese conduc la formarea altor corpuri discrete care la rândul lor pot suferi mișcări, interacțiuni, deformări și fracturări. Aplicația Geomechanica IRAZU cu ajutorul căreia au fost efectuate simulările din această lucrare este are ca principiu de calcul metoda FDEM, fiind astfel orientată pentru simulări specifice mecanicii rocilor. În lucrare am prezenta o simulare la forfecare după un plan obligat pentru lignit. Pentru aceasta am prezentat o serie de noțiuni teoretice legate de acest tip de solicitare, metode standardizate de forfecare, precum și pașii care trebuie urmați pentru simularea solicitării la forfecare.

Florin Dumitru POPESCU, PhD Eng. Habil., Professor, University of Petroșani, Department of Mechanical, Industrial and Transport Engineering, fpopescu@gmail.com, 072371930320 Universității street, 332006, Petroșani, HD.
Ciprian-Gheorghe DANCIU, PhD Eng., Assoc. Prof., University of Petroșani, Department of Mining Engineering, Topography and Construction, CiprianDanciu@upet.ro, 0726351238.
Andrei ANDRAȘ, PhD Eng. Habil, Assoc. Prof., University of Petroșani, Department of Mechanical, Industrial and Transport Engineering, andrei.andras@gmail.com, 0722366653.
Ildiko BRÎNAȘ, PhD Eng., Lecturer, University of Petroșani, Department of Mechanical, Industrial and Transport Engineering, kerteszildiko@ymail.com, 0726703067.
Sorin Mihai RADU, PhD Eng., Professor, University of Petroșani, Department of Mechanical, Industrial and Transport Engineering, sorin_mihai_radu@yahoo.com, 0722642340.
Ancuța Mirela NEAGA (RADU), PhD student Petroleum – Gas University of Ploiesti, Engineer, National Institute of Research and Development for Safety in Mines and Explosion Protection – INSEMEX Petroșani, mirela.radu@insemex.ro, 0723170642, 32-34 Gen. Vasile Milea street, 332047, Petroșani, HD.